Polymer Bulletin 34, 493–500 (1995)

Polymer Bulletin

Blends of poly(ethylene oxide) with chitosane acetate salt and with dibuturylchitin: Structure and morphology

A. Wrzyszczynski [1], Xia Qu [2], L. Szosland [3], E. Adamczak [4], L. Å. Lindén [4], J. F. Rabek [4]

[1] Department of Chemistry, Technical and Agriculture University, Seminaryjna 3, PL-85326 Bygoszcz, Poland

[2] Department of Materials Science and Engineering, University of Science and Technology of China, Heifei, Anhui, China

[3] Department of Physical Chemistry of Polymers, Technical University, Zeromskiego 116, PL-90543 Lódz, Poland

[4] Polymer Research Group, Department of Dental Biomaterials, Karolinska Institute (Royal Academy of Medicine), Box 4064, S-141 04 Huddinge, (Stockholm), Sweden

Received: 27 December 1994/Accepted: 23 January 1995

SUMMARY

This paper presents the results of a study of the chemical structure and morphology of polyblends of chemically modified chitin and chitosane with poly(ethylene oxide). Poly(ethylene oxide)(PEO) forms a compatible one-phase blend with chitosane acetate salt (PEO/CHIACA) and a non-compatible two phase blend with dibutyrylchitin (PEO/DBCHI). The compatible one-phase blend of PEO/CHIACA is formed due to the formation of strong hydrogen bonds between ether groups in PEO and hydroxy groups in CHIACA. Chemical and crystalline morphological structure is discussed here.

INTRODUCTION

Chitin is one of the most abundant biopolymers being second only to cellulose in the amount produced annually by biosynthetis [1]. It occurs in animals, particularly in crustacea, molluscs and insects, where it is an important constituent of the exoskeleton, and in certain fungi where it is the principal fibrillar polymer in the cell wall [2].

Chitosane is a product obtained by alkaline deacetylation of chitin [3] but its natural occurrence is much less widespread than chitin.

Both chitin and chitosane and their chemically modified analogues exhibit very good biocompatibility [4,5]. Gel-forming modified chitosanes are more suitable for medical use than chitosane itself [6,7]. Chitosane has also been investigated in association with dental materials such as poly(tetrafluorethylene) [8], microvascular prothesis [9], hydroxyapatite [10], and in dental surgery [11] and it was found that it improved biocompatibility, favoured cell migration, and inhibited adsorption of oral streptococci [12]. Chitosane also exhibits haemostatic and bacteriostatic action (13-15) and is used for plaque inhibition and denture cleansing [16,17].

Our earlier interest was in the application of chitosane-poly(acrylic acid) for tightening of microchannels in teeth [18]. Poly(ethylene oxide) form polyblends with modified chitin and chitosane. The formed complex could be applied in the form of thin films for wound dressing or even as biodegradable material for food packing. Poly(ethylene oxide) films are biocompatible and exhibit a low degree of protein absorption and cell adhesion [19-24]. For this reason, we have chosen to study the structure and morphology of blends of poly(ethylene oxide) with chitosane acetate and dibutyrylchitin.

EXPERIMENTAL

A commercial chitosane (CHI) of low molecular weight 70,000 was obtained from Fluka (Swiss). Poly(ethylene oxide) (PEO) type WSRN 750 produced by Union Carbide was used without further purification. Chitosane acetic acid (CHIC) and dibutyrylchitin (DBCHI) were prepared according to the literature [3] and [25,26], respectively. Polyblends of PEO/CHIACA and PEO/DBCHI were prepared from 3 wt-% solutions of components in water and nitromethane, respectively.

IR absorption spectra of CHIACA, DBCHI and their blends with PEO were recorded from the films using a FTIR spectrometer, Model 1650, Perkin Elmer.

DSC curves were obtained using a Perkin Elemer DSC 4 thermal analysing system with a standard heating and cooling rate of 10^{o} C min^{-1}; 3-4 mg samples were used in a nitrogen atmosphere over the temperature range 25-300°C. Indium (T_m = 156.6°C) was used for temperature calibration.

Wide angle X-ray diffraction (WAXD) patterns were obtained using a wide angle X-ray diffractometer type HZG 4/A-2 (Germany) (CuK_α-tube and Ni Filter). The diffraction patterns were determined over a range of diffraction angles $2\theta = 10^{o}$-30^{o}. Polarized optical and scanning electron microscope (SEM) photomicrographs were made with a Nikon polarizing microscope, type Optophot-2 Pol and with a Jeol JSM - 820 scanning microscope, respectively.

RESULTS AND DISCUSSION

Chitin (2-acetoamid)-2-deoxy-(1-4)-β-D-glycopyranan) and chitosane (2-amino-2-deoxy-(1,4-)-β-D-glycopyranan) (CHI) are practically insoluble in water and organic solvents due to its micelle structure, the close packing of their molecular chains, and the presence of several different types of hydrogen bonding. In order to increase their solubility, they have to be chemically modified. Chitosane gives water-soluble salts with acetic acid (CHIACA) [3], whereas dibutyrylchitin (DBCHI) [26] is easily soluble in dioxane, tetrahydrofuran, acetone, nitromethane, DMF, methanol, and other common solvents.

Polyblends of poly (ethylene oxide) (PEO) with chitosane acetic salt (PEO/ CHIACA) and dibutyrylchitin (PEO/DBCHI) casted from water and nitromethane (3wt -% solutions) respectively, form clear (transparent) to opaque (non-transparent) films. Their transparency is dependent on the polyblend composition and is due to the presence of spherulitic structures and its one- or two-phase crystalline morphology.

The scanning electron microscopy (SEM) microphotographs show that PEO/CHIACA give very compatible blends (Fig1-I), whereas PEO/DBCHI blends are incompatible (Fig.1-II). In the last case it is possible to observe complete separation of the phases of the components (PEO and DBCHI) in the blends (Fig.2). The good compatibility of PEO with CHIACA is probably due to the formation of hydrogen bonds between OH groups and CHIACA and ether links in PEO.

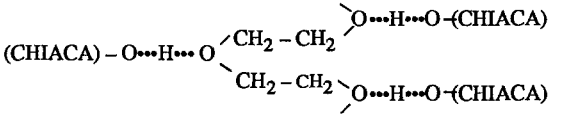

The butyrylic groups, which almost completely replace the OH groups in DBCHI, play the role of spatial hindrance, rendering formation of a one-phase compatible blend with PEO (Fig.2).

Pure PEO films crystallize according to a spherulitic morphology. When PEO films are observed under the polarizing microscope, with crossed polaroids, circular birefringent regions, truncated by impingements are observed. The birefrigent patterns display a Maltese cross with arms parallel to the directions of the polarize and analyzer. (Fig.3).

Polarized optical microphotographs show that the radius of PEO spherulites crystallized from water (Fig.4-IA) are larger than those crystallized from nitromethane (Fig.4-IIA).

Addition of CHIACA and DBCHI to PEO causes different changes in the spherulitic morphology of PEO depending on the type and ratio of the components in the blends (Fig 4). In the case of PEO/CHIACA blends, spherulite structures are formed up to PEO :CHIACA ratio 50:50 (Fig. 4-IC) and disappear completely at a ratio of 25:75 (Fig. 4-ID).

For PEO/DBCHI blends the last spherulite structures were observed at ratio 80:20 (Fig.4-IIB), whereas they completely disappear at a ratio of 75:25. The regular spherulites observed in pure PEO (Fig.4-IA) are distorted in its blends with CHIACA (Figs. 4-IB and 4-IC) and with DBCHI (Fig. 4-IIB).

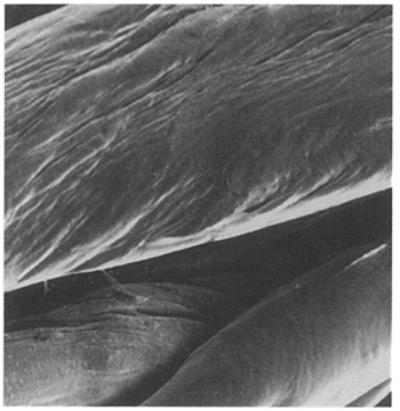

IA

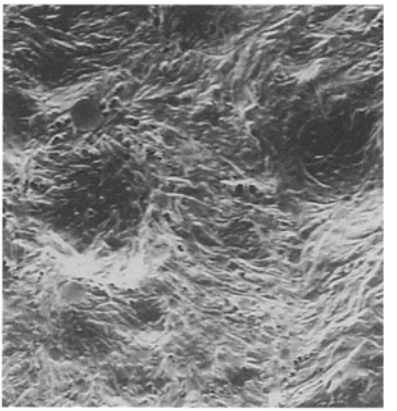

IIA

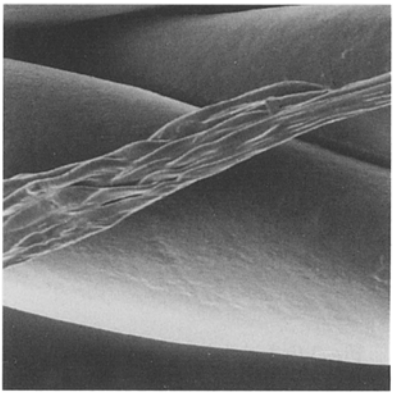

IB

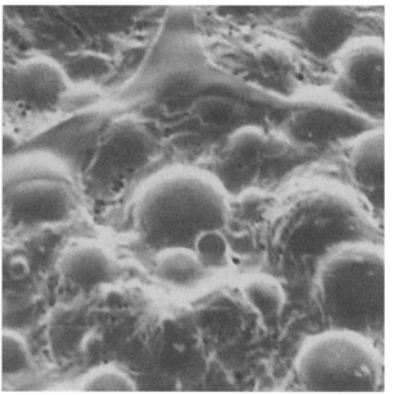

IIB

IC

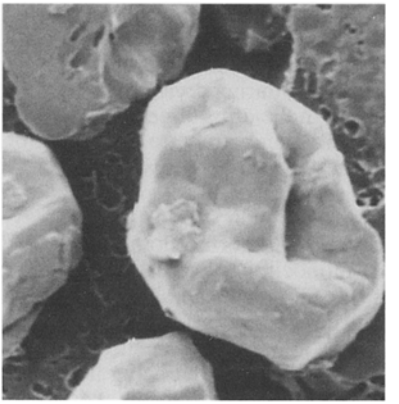

IIC

Fig.1 SEM microphotographs of blends of: (I) PEO/CHIACA and (II) PEO/DBCHI at different ratios; (IA) and (IIA)=75:25; (IB) and (IIB) = 50:50; (IC) and (IIC)= 25:75. Magnification 2000x.

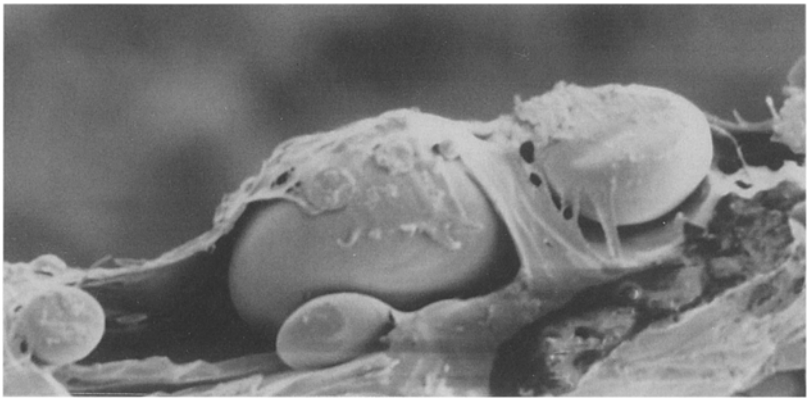

Fig.2 SEM microphotograph of the incompatible PEO/DBCHI blend at ratio 50:50. The egg-like morphology belongs to the DBCHI imbedded in PEO matrix. Magnification 3000x.

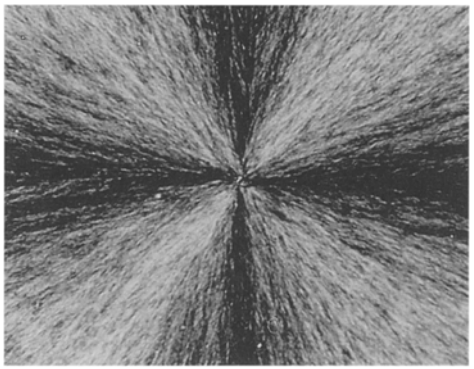

Fig.3 Polarisation microscope image of PEO spherulite with birefringent pattern displaying a Maltese cross Magnification 300x.

This observation indicates that growth of spherulites in PEO matrix depends on a phase segregation phenomen, which is the largest in incompatible PEO/DBCHI and much smaller in compatible PEO/CHIACA. In the last case, CHIACA molecules are probably incorporated, during crystallization, in interlaminar regions of PEO.

The PEO in the crystalline state (70-80% of crystallinity in our sample) has the tendency to form a helical structure consisting of a succession of nearly trans, and gauche forms about the C-C, O-C, and C-C bonds, respectively [27-30]. Chitin [2,31] and chitosane [2,32] form structurally complicated crystalline polyamorphic (α,β and γ-) forms, depending on their origin, and the way of preparation. The α-form of chitin, due to the symmetry of the orthorhombic cell, differs from the β-form of chitin in which the unit cell is monoclinic, whereas γ-form may contain both types of cells. The most abundant form is α-chitin, which also appears to be the most stable since both the β- and γ-chitin may be converted into the α-form by a suitable treatment. In both chitin and chitosane the chains are arranged in sheets or stacks, the chains in any one sheet having the same direction or "sense" and being hydrogen-bonded together through $C(2_1)N\text{-}H\bullet\bullet\bullet O{=}C\ (7_3)$ bonds. In β-chitin there is an additional $C(6_1')OH\bullet\bullet\bullet O{=}C(7_3)$ intra sheet hydrogen bond between two adjacent chains. Both chitosane and DBCHI have an orthorhombic arrangement with unit cells of a =8.9Å, b =17.0 Å, and c =10.25Å (fibre axis) [32,33] and a =4.4Å, b =13.4 Å and c =10.3 Å (fibre axis) [34], respectively.

The WAXD patterns show that PEO (Fig.5A) and DBCHI (Fig.5G) have crystalline morphology, whereas CHIACA is completely amorphous (Fig.5D).

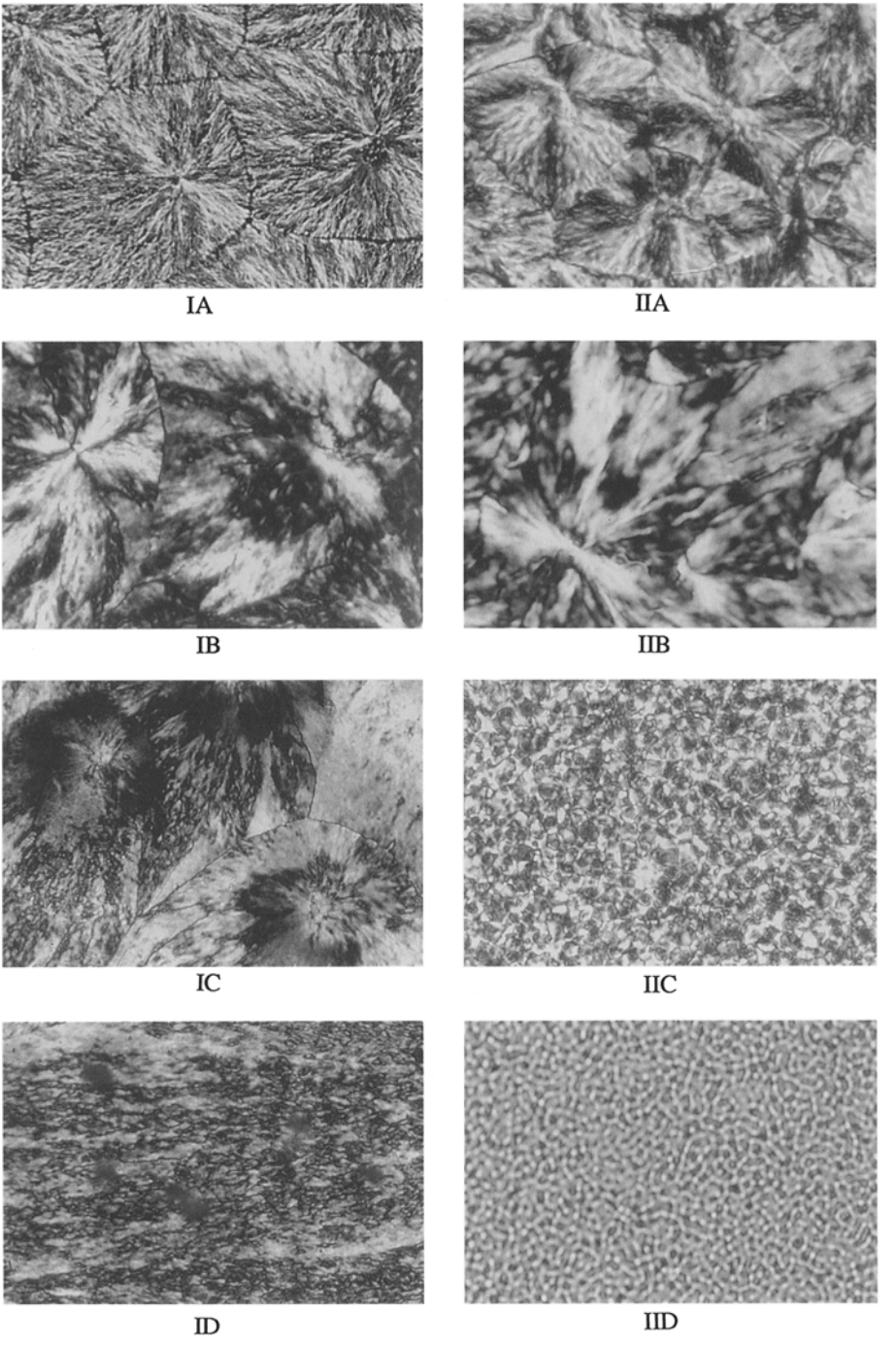

Fig. 4 Polarizing microscope microphotographs of: IA and IIA pure PEO crystallized from water and nitromethane respectively; and blends of PEO/CHIACA at ratio: (IB) 75 : 25; (IC) 50 : 50; (ID) 25 : 75; PEO/DIBCHI at ratio: (IIB) 80:20, (IIC) 50: 50 and (IID) 25 : 75.

The PEO crystallizes in PEO/CHIACA (Fig.5C) and PEO/DBCHI (Fig.5F) blends evenly at a ratio 25:75. The PEO crystallization in PEO/CHIACA and PEO/DBCHI blends is probably very little influenced by the CHIACA or DBCHI component. However, some of the CHIACA and DBCHI molecules can be trapped between the growing fibrils and cause distortion of the growing spherulites (Fig,4-I and 4-II).

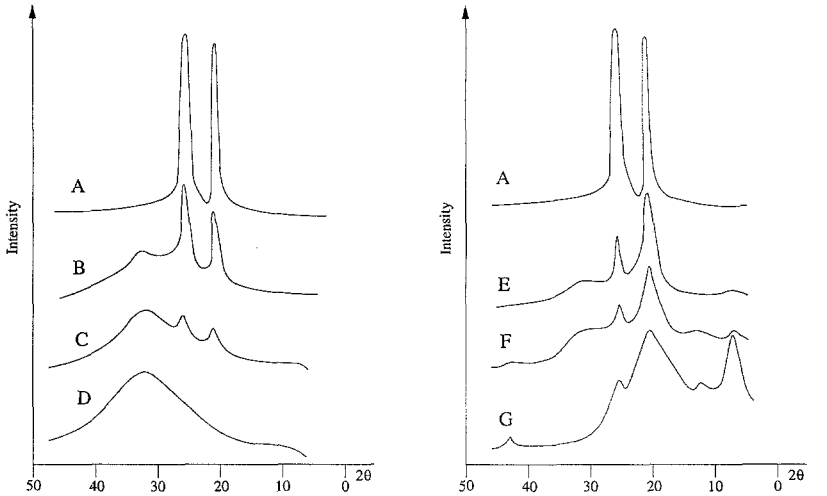

Fig. 5 WAXD diffraction patterns of: (A) pure PEO; (D) pure CHIACA; (G) pure DBCHI, and blends of PEO/CHIACA at ratio: (B) 50:50; (C) 25:75; and blends of PEO/DBCHI at ratio: (E) 50:50; (F) 25:75.

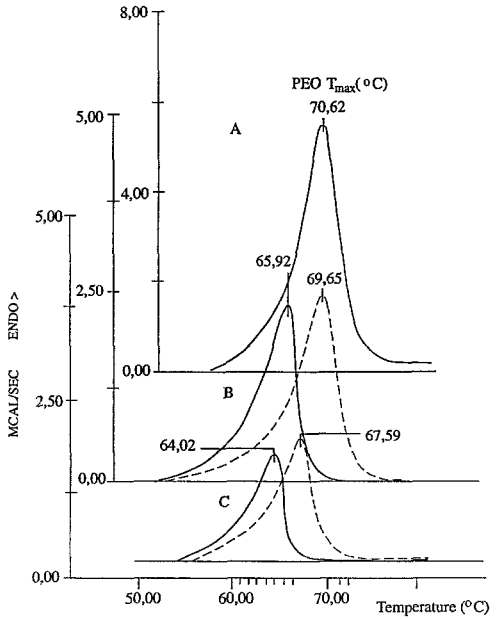

Fig. 6 DCS curves of: (A) pure PEO and blends of PEO/CHIACA at ratio: (B) 50:50 (C) 25:75; and PEO/DBCHI (---) at ratio: (D) 50:50 and (E) 25:75.

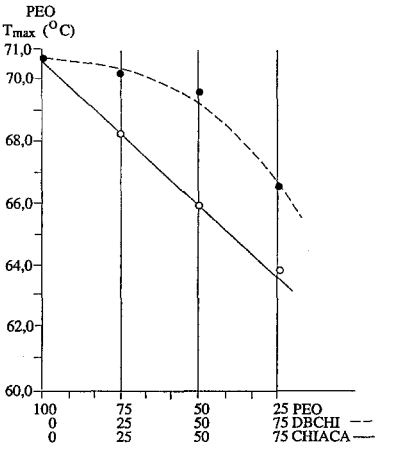

Fig.7 Shifting of the melting temperature of PEO in blends: PEO/CHIACA (- - -) and PEO/DBCHI (—) at different ratios.

The DSC curves show that the melting temperatures (T_{max}, °C) of PEO/CHIACA and PEO/DBCHI blends decrease with increasing content of CHIACA or DBCHI in a blend (Fig. 6 and Fig.7). The decreasing T_{max} is linearly only for PEO/CHIACA blend but not for PEO/DBCHI (Fig.7). This variation can be due to the diluent effect of the CHIACA or DBCHI on the chemical potential of the crystallizable PEO as the two components are blended The spherulities of the crystallizable PEO component grow in a matrix of another blend's component.

The DSC curves of crystalline DBCHI (curves are not given here) show existence of the endothermic minimum partition in the vicinity of 75°C, similar to that reported elsewhere [34]. However, glass transition temperatures (T_g) in the range 150-250°C were not found. The CHIACA and DBCHI start to decompose at temperatures of 125°C (brown) to 215 °C (black) and 210 °C (brown) to 250 °C (black) respectively.

The FTIR spectra of PEO (Fig.8A), CHIACA (Fig.8B) and DBCHI (Fig. 8D) and their blends PEO/CHIACA (50:50) (Fig.8C), and PEO/DBCHI (50:50) (Fig.8E) show that they are almost superimposed (Fig.8 ABC and Fig.8 ADE)

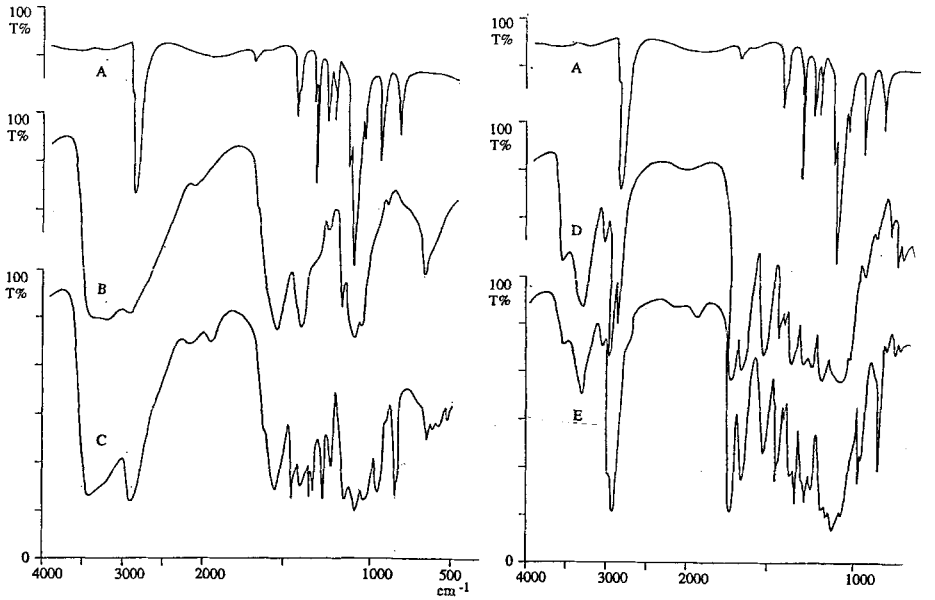

Fig.8 FTIR spectra of: (A) pure PEO; (B) pure CHIACA; (D) pure DBCHI and blends of: (C) PEO/CHIACA 50:50; (E) PEO/DBCHI 50:50.

IR spectra of CHIACA (Fig.8B) and DBCHI (Fig.8D) differ from each other and are interpreted elsewhere [25,34,35]. In the case of PEO/CHIACA, a band at 3250cm^{-1} is formed (Fig.8C). This is attributed to the formation of intermolecular hydrogen bonds between OH groups in CHIACA and ether links in PEO. The strong band at 1564 cm^{-1} attributed to $-NH_3^+$ ($^-$OOC-) in CHIACA (Fig.8B) also exists in PEO/CHIACA (Fig.8C), showing that it does not participate in the intermolecular bonding between PEO and CHIACA.

In conclusion, only the compatible PEO/CHIACA blend may be considered for application as wound-dressing film in medicine and as a packaging-film material.

ACKNOWLEDGEMENTS

The authors gratefully acknowledge the support of the Swedish Institute, Stockholm, which generously provided a post-doctorate stipendium for Dr A.Wrzyszczynski.

REFERENCES

1. Tracey MV (1957) Rev Pure Chem 7 :1
2. Roberts GAF (1992) Chitin chemistry, MacMillan, London
3. Avstin RP Sennet S (1986) in Muzzarelli RAA Jeuniaux C Gooday GM (eds) Plenum New York p 279
4. Daly WH (1991) in Polymers from biobased materials, Noyes Data, Park Ridge
5. Sandford PA Steinnes A (1991) in McCornick CC Butler GB (eds) Water-soluble polymers, ASC Symp Ser 467 p 430
6. Muzzarelli RAA (1988) Carbohyd Polym 8:1
7. Muzzarelli RAA Biagini G Damedei A Pugnalom A Dalio J (1992) in Crescenzi V Stivala SS (eds) Industrial polysaccharides: biomedical and biotechnology advances, Gordon Breach, New York p 77
8. Sakai M (1987) US Pat 4 803 078
9. Van Der Lei B Wildevuur CHR (1989) Plast Reconst Surg 84 : 960
10. Ito M (1991) Biomater 12:41
11. Muzzarelli RAA Biagini G Bellardini M Simonelli L Castaldini C Fratto G Biomater 14:38
12. Sano H Matsukubo T Itoh H Takaesu Y (1987) J Dent Res 66 : 141
13. Shibazaki K Matsukubo T Sugihara N Tashiro E Tanabe Y Takaesu Y Kokubyo Gakki Zasshi 38 : 572
14. Itoh H Okubo S Sano H Shibazaki K (1987) Jpn Kokai Tokkyo Koho 62:248 468
15. Muzzarelli RAA Tarsi P Fillipini O Gioranetti E Biagini G Varaldo PE (1990) Antimicrob Agents Chemother 34:2019
16. Komiyama N Ito H (1988) Jpn Kokai Tokkyo Koho 63:14 414
17. Komiyama N Hitoi H Sano N (1984) Ger Offen DE 3 343 200
18. Lindén LÅ Adamczak E Morge S Wrzyszczynski A (1994) in Proc 6th Int. Conf Chitin Chitosan, Gdynia, Poland (in print)
19. Park KD Okano T Nojiri C Kim SW (1988) J Biomed Mater Res 22:977
20. Jacobs HA Okano Y Kim SW (1989) J Biomed Mater Res 23:611
21. Maechling-Strasser C Dejardin P Galin JC Schmidt A (1989) J Biomed 23:1385
22. Brinkman E Poot A van de Does L Bantjes A (1990) Biomater 11:200
23. Desai NP Hubbell JA (1991) J Biomed Mater Res 25:829
24. Gombotz WR Guanghui W Horbett TA Hoffman AS (1991) J Biomed Mater Res 25:1547
25. Kaifu H Nishi N Komasi T Tokura S Somorin O (1981) Polym J 13:241
26. Szosland L (1994) Sci Bull Lodz Techn Univ p 45
27. Koenig J Angood AC (1970) J Polym Sci Phys Ed 8:1787
28. Miyazawa T (1961) J Chem Phys 35:693
29. Tadekoro H Yoshihara T Chatani Y Tahara S Murashi S (1964) Makromol Chem 73:109
30. Takahashi Y Tadekoro H (1973) Macromol 6:672
31. Rudall KM (1963) Adv Insect Physiol 1:257
32. Ogawa K Hirano S Miyanishi T Yui T Watanabe T (1984) Macromol 17:973
33. Samuels RJ (1981) J Polym Sci Phys Ed 19:1081
34. Urbanczyk J Lipp-Symonowicz B Jeziorny A Urbaniak-Domagala W Wrzosek H (1984) J Appl Polym Sci 53:1469
35. Peng De Yao K Yuan C Goosen MFA (1994) J Polym Sci Chem Ed 32:591